Light-scattering analysis of the temperature-dependent transmittance of a polymer-dispersed liquid-crystal film in its isotropic phase

G. Paul Montgomery, Jr. and Nuno A. Vaz
Department of Physics, General Motors Research Laboratories, Warren, Michigan 48090-9055
(Received 18 May 1989; revised manuscript received 7 August 1989)

We have measured the temperature-dependent transmittance of a polymer-dispersed liquid-crystal (PDLC) film in its isotropic phase. We show that the measured transmittance can be quantitatively described within experimental error over a wide temperature range using Rayleigh-Gans light-scattering theory with film parameters previously determined from refractive-index studies and scanning electron microscopy; no freely adjustable parameters or normalization constants are necessary to describe the measured transmittance data. We obtained equally good agreement between theory and experiment regardless of whether or not we included droplet correlation effects in our transmittance calculations. The precision with which the refractive index of the matrix material in a cured PDLC film can be determined is the main factor preventing us from quantitatively assessing the role of droplet correlation effects in PDLC films at this time. We have also compared the transmittance characteristics of our PDLC film with the published transmittance of a film composed of liquid crystal in the pores of a solid matrix. We find that the published results are consistent with the form of the equations of scattering theory; however, quantitative agreement between measured and calculated transmittance would require film parameters different from those published.

I. INTRODUCTION

Polymer-dispersed liquid-crystal (PDLC) films, consisting of liquid-crystal (LC) microdroplets dispersed in polymer matrices, are potentially useful for a variety of electro-optic applications because they can be switched electrically from a cloudy, light-scattering state to a transparent state.[1-7] Optimizing the light-scattering performance of a PDLC film for a specific application requires control over various film parameters including the refractive indices of the liquid-crystal and polymer matrix materials and the concentration and size distribution of the liquid-crystal droplets in the film.[8-15] In a previous paper,[8] we showed that the variation in PDLC film transmittance with temperature can be understood qualitatively in terms of the temperature dependence of the refractive indices of the film components. In particular, we argued that PDLC film transmittance in the isotropic phase depends weakly on temperature because the refractive indices of the LC and matrix materials vary with temperature at approximately the same rate. In this paper we use Rayleigh-Gans (RG) light-scattering theory[16-18] to calculate the temperature-dependent transmittance of a PDLC film in its isotropic phase, using as input data all the individual film parameters which we have measured. We will show that the magnitude of the transmittance, as well as its weak-temperature variation, are well described by these calculations.

Although Rayleigh-Gans (RG) light-scattering theory has recently been extended to optically anisotropic droplets,[11] we have chosen in this study to focus on the isotropic phase of our PDLC films rather than the anisotropic nematic phase for several reasons. For the isotropic phase we can use RG scattering theory for optically isotropic scatterers; this theory has been thoroughly tested and its strengths and limitations are well understood.[16-18] In the nematic phase we would have had to use the extended RG theory which has not yet been fully tested experimentally. In addition, in the nematic phase, some liquid-crystal refractive indices are such that the conditions needed for valid application of RG theory will be only marginally satisfied for the droplet sizes found in many PDLC films. Finally, multiple scattering cannot validly be neglected in the nematic phase of PDLC films, particularly in the off state,[19] except for low concentrations of very small droplets.[12] Therefore we felt that it was best to apply RG theory to PDLC films under conditions where it could be expected to be valid, where complications of optical anisotropy were not present, and where multiple scattering effects could validly be neglected. Computation of PDLC film transmittance at temperatures above the nematic to isotropic phase transition temperature T_{NI} was a problem which met all these requirements. Failure of the calculations to account for our experimental observations in this case would have raised serious doubts about the applicability of RG theory to PDLC films under any conditions. On the other hand, successful application of the theory in this case would help to validate many of the conclusions reached in a variety of independent measurements which have been performed on PDLC films in several laboratories. Calculations for the isotropic phase can also provide useful information about the sensitivity of calculated scattering characteristics to variations in key film parameters. Such information will be useful in comparing predictions of the extended RG theory with measurements on PDLC

 ©1989 The American Physical Society

films in their nematic phase.

Another motivation for this work is the fact that the temperature dependence of PDLC film transmittance in the isotropic phase which we have measured in our laboratory differs significantly from that reported[20] by Aliev for a system consisting of liquid crystal in its isotropic phase in the pores of a solid matrix. The transmittance of the PDLC film increases by only a few percent over a 50 °C temperature range whereas the transmittance of the Aliev system decreases significantly over a 30 °C range. We wished to investigate whether or not these differences in behavior could be explained in terms of light-scattering theory and differences in the material parameters of the two systems.

II. TRANSMITTANCE OF A LIGHT-SCATTERING FILM IN THE RAYLEIGH-GANS APPROXIMATION

A. Basic theory

We shall use the Rayleigh-Gans (RG) approximation for light scattering by a system of spherical particles[16] to describe the effects of light scattering by the liquid-crystal microdroplets on the transmittance of our PDLC film. For this approximation to be valid, two conditions must be satisfied,

$$|m-1| \ll 1 , \tag{1}$$

$$2ka|m-1| \ll 1 . \tag{2}$$

In these equations, $k=2\pi n_p/\lambda$ is the magnitude of the wave vector of the incoming radiation inside the polymer matrix, λ is the vacuum wavelength of this radiation, a is the radius of a liquid-crystal droplet, and m, the relative refractive index, is defined in terms of the liquid-crystal refractive index n_{LC} and the polymer matrix refractive index n_p by

$$m=\frac{n_{\mathrm{LC}}}{n_p} . \tag{3}$$

Provided that multiple scattering can be neglected, the transmittance τ of a PDLC film cured between two glass plates can be written to good approximation as[17,18]

$$\tau=(1-R)^2 e^{-\kappa d} , \tag{4}$$

where d is the film thickness, κ is an extinction coefficient to be discussed below, and R is the reflectance at a single air-glass interface. (For our measurements, which were performed at normal incidence, $R \approx 0.04$.) It is generally agreed that, if κd is below about 0.1, multiple-scattering effects can be neglected in a transmittance measurement.[16] For $\kappa d=0.1$, the transmittance τ will be 0.834 when $R=0.04$. Since the transmittance of our sample (see Sec. IV) is about 0.83, neglect of multiple scattering in our transmittance analysis is justified.

The extinction coefficient κ is given by[17,18]

$$\kappa=N_v \sigma_{\mathrm{ext}} , \tag{5}$$

where N_v is the average number of liquid-crystal droplets per unit volume and σ_{ext} is the extinction cross section for a single droplet. Since the liquid crystal in the droplets is nonabsorbing at 589 nm, the extinction cross section of a droplet σ_{ext} is identical with the scattering cross section σ_s at this wavelength. In Appendix A we show that the extinction cross section for a collection of nonabsorbing RG particles may be written in the form

$$\sigma_{\mathrm{ext}}=\sigma_s^{\mathrm{eff}}=\pi a^2 |m-1|^2 \Phi^{\mathrm{eff}}(ka) , \tag{6}$$

where

$$\Phi^{\mathrm{eff}}(ka)=\tfrac{4}{9}(ka)^4 \int_0^{\pi} (1+\cos^2\theta_s) \left[\frac{3}{(k_s a)^3} (\sin k_s a - k_s a \cos k_s a) \right]^2 [1+\beta N_v \hat{h}(k_s,\eta,a)] \sin\theta_s \, d\theta_s . \tag{7}$$

The factor β in this equation is given by

$$\beta=\begin{cases} 0, & \text{for independent scattering} \\ & \text{(no correlation effects) ;} \\ 1, & \text{if droplet correlation effects} \\ & \text{are important .} \end{cases} \tag{8}$$

In this paper we shall compute film transmittance both with and without droplet correlation effects. In the calculations with correlation, we shall use the Percus-Yevick approximation for a system of hard spheres[21] to compute the function $\hat{h}(k_s,\eta,a)$, as discussed in Appendix B. This approach allows us to perform our calculations for the high droplet concentrations often found in PDLC films.

Finally, since the average number of droplets per unit volume N_v is related to the volume fraction η occupied by the droplets by

$$N_v=\frac{\eta}{(\frac{4}{3}\pi a^3)} , \tag{9}$$

we obtain from Eq. (4)–(6) and (9),

$$\tau=(1-R)^2 \exp\left[-\left[\frac{3\eta d}{4a} \right] (m-1)^2 \Phi^{\mathrm{eff}}(ka) \right] . \tag{10}$$

This equation, with $\Phi^{\mathrm{eff}}(ka)$ given by Eq. (7), is the basic relation describing film transmittance in terms of light scattering.

In Sec. II B, we consider the temperature dependence of the individual parameters in Eq. (10). This will allow us to identify those parameters which contribute most significantly to the temperature dependence of film transmittance and to rewrite Eq. (10) in a form that is convenient for comparison with experimental temperature-dependent transmittance data.

B. Temperature dependence

As the temperature of a PDLC film increases, both the matrix material and the droplets will expand. These changes can be described by the coefficients of volume expansion of the liquid crystal and the polymer matrix. These coefficients, derived from the measured refractive indices of the materials in our PDLC film and their rates of change with temperature,[8] are listed in Table I. Using these values one can show that the droplet radius a and the film thickness d will each increase by $<2\%$ over the temperature range from 40 to 90 °C.

The refractive indices of the liquid crystal and polymer matrix decrease linearly with temperature,[8]

$$n_{\mathrm{LC}}(T)=n_{\mathrm{LC}}(T_0)+(T-T_0)\left.\frac{dn_{\mathrm{LC}}}{dT}\right|_{T_0} \tag{11}$$

and

$$n_p(T)=n_p(T_0)+(T-T_0)\left.\frac{dn_p}{dT}\right|_{T_0} . \tag{12}$$

Using the values given in Table I we find that, although n_{LC} and n_p individually change by only a few percent as the temperature increases from 40 to 90 °C, the difference $|m-1|$ will change by approximately 40%.[24] Therefore, any temperature dependence in the transmittance of our PDLC film will be due almost entirely to the temperature dependence of the factor $|m-1|^2$ in Eq. (10).

If we assume that the temperature dependence of film transmittance is due only to the factor $|m-1|^2$, we can rewrite Eq. (10) in a form which clearly reveals the dependence of transmittance on temperature,

$$\tau=(1-R)^2\exp[-(c_1+c_2T)^2] . \tag{13}$$

In this equation, c_1 and c_2 are constants which depend on material and geometric parameters but not on temperature,

$$c_1=\frac{1}{n_p(T_0)}\left[\left[\frac{3\eta d}{4a}\right]\Phi^{\mathrm{eff}}(ka)\right]^{1/2}\left[(n_{\mathrm{LC}}(T_0)-n_p(T_0)-\left[\left.\frac{dn_{\mathrm{LC}}}{dT}\right|_{T_0}-\left.\frac{dn_p}{dT}\right|_{T_0}\right]\right] , \tag{14}$$

$$c_2=\frac{1}{n_p(T_0)}\left[\left[\frac{3\eta d}{4a}\right]\Phi^{\mathrm{eff}}(ka)\right]^{1/2}\left[\left.\frac{dn_{\mathrm{LC}}}{dT}\right|_{T_0}-\left.\frac{dn_p}{dT}\right|_{T_0}\right] . \tag{15}$$

For analysis of experimental temperature-dependent transmittance data, it is convenient to rewrite Eq. (13) as

$$\left[-\ln\left[\frac{\tau}{(1-R)^2}\right]\right]^{1/2}=c_1+c_2T . \tag{16}$$

This equation will be used to analyze new transmittance data for a PDLC film (Sec. IV) and published data for the porous film of Aliev[20] (Sec. V).

III. CALCULATIONS AND INPUT PARAMETERS

A. Calculations

Calculation of film transmittance at a fixed temperature would be straightforward provided the size distribution of the liquid-crystal droplets, the volume fraction occupied by the droplets, the thickness of the film, and the refractive indices of both the liquid-crystal and the polymer matrix materials were all known precisely. Temperature dependence could be included if the rates of change of the LC and matrix refractive indices with temperature were known. The calculations could be performed either using Eq. (10), with $\Phi^{\mathrm{eff}}(ka)$ given by Eq. (7), or using Eq. (13), with c_1 and c_2 given by Eqs. (14) and (15).

In practice, the calculation of film transmittance for comparison with experiment is complicated by the fact that there are different degrees of uncertainty in our knowledge of the parameters in the scattering equations. These uncertainties, which must be considered in any meaningful comparison of calculations with experiment,

TABLE I. Properties of materials used in PDLC sample. All data in this table are from Ref. 8.

Material	n(25 °C)	$10^4\frac{dn}{dT}$(25 °C) (°C^{-1})	Correlation coefficient	$10^4\beta_0^{GD}$ (°C^{-1})[a]	$10^4\beta_0^{LL}$ (°C^{-1})[b]
7CB[c]	1.5785[d]	−4.300[d]	0.9997	7.433	6.078
Devcon 5A[e]	1.5723[f]	−3.756[f]	0.9995	6.562	5.382
Devcon 5B[e]	1.5406[f]	−3.474[f]	0.9996	6.885	5.820
Devcon 5A: Devcon 5B 1:1	1.5700[f]	−3.559[f]	0.9951	6.149	5.126

[a]Coefficient of volume expansion obtained by using Gladstone-Dale model to relate refractive index to density (see Ref. 8).
[b]Coefficient of volume expansion obtained by using Lorentz-Lorenz model to relate refractive index to density (see Ref. 8).
[c]See Ref. 22.
[d]From linear regression analysis of refractive index data in isotropic phase.
[e]See Ref. 23.
[f]From linear regression analysis of refractive index data.

will be discussed in Sec. III B 1 on input parameters.

Because transmittance calculations that take experimental uncertainty into account can be complex and time consuming, it is desirable to screen experimental data to determine whether or not detailed calculations are justified. We used Eq. (16) as the basis for a simple procedure to do this. We allowed c_1 and c_2 to be freely adjustable fitting parameters and used linear regression procedures to obtain the best fits of our experimental transmittance data to Eq. (16). If good fits could not be obtained by this procedure, which imposed no constraints on c_1 and c_2, it is obvious that good agreement would not be obtained from a transmittance calculation in which c_1 and c_2 were computed from experimental data. Failure to obtain good fits with the unconstrained linear regression procedures would imply that the experimental transmittance data were inconsistent with the general form of the equations of scattering theory and further transmittance calculations would be meaningless.

On the other hand, it is apparent that unconstrained linear regression analysis could produce a good fit to the experimental data with coefficients c_1 and c_2 which were inconsistent with reasonable values of n_{LC}, n_p, $(dn_{\mathrm{LC}}/dT)|_{T_0}$, $(dn_p/dT)|_{T_0}$, d, η, and a. Therefore, a good fit at this stage would ensure only that the experimental transmittance data were consistent with the form of the equations of RG light-scattering theory and that further calculations were justified.

If unconstrained linear regression did give a good fit to a set of experimental transmittance data, we then used constrained simplex minimization procedures[25] to compute film transmittance from Eq. (10) while allowing for uncertainty in our knowledge of n_{LC}, n_p, $(dn_{\mathrm{LC}}/dT)|_{T_0}$, $(dn_p/dT)|_{T_0}$, d, η, and a. To do this, we allowed these quantities to be fitting parameters in the calculation; however, we constrained each parameter to vary only over a limited range determined either by the precision with which we could measure it directly or by our ability to extract its value from experimental data, as discussed in Sec. III B 1. In view of the discussion in Sec. II, we considered only the temperature dependence of the refractive indices n_{LC} and n_p; changes in a and d with temperature were neglected in all simplex minimizations. Computations were performed both with $\beta=0$ (independent scattering—no droplet correlation effects) and with $\beta=1$ (droplet correlation effects included).

B. Input parameters

1. PDLC film

Column 2 of Table II shows the ranges over which the parameters n_{LC}, n_p, $(dn_{\mathrm{LC}}/dT)|_{T_0}$, $(dn_p/dT)|_{T_0}$, η, and a were allowed to vary in our calculation of PDLC film transmittance. Where appropriate, measured or estimated values of the parameters are also given (column 3). We note that the assumptions required for valid use of the RG approximation, viz., Eqs. (1) and (2), are satisfied for all combinations of film parameters used in the calculations.

(a) *Liquid-crystal refractive index and its temperature dependence.* We have measured precisely the values of n_{LC} and $(dn_{\mathrm{LC}}/dT)|_{T_0}$ for the pure LC material 7CB.[8,22] However, differences between the isotropic-nematic phase transition temperature of a pure liquid crystal and the liquid crystal in the droplets of a PDLC film indicate that some polymer precursors remain dissolved in the liquid crystal after polymerization.[2,3,10] As a result, there is a small uncertainty in the parameters n_{LC} and $(dn_{\mathrm{LC}}/dT)|_{T_0}$ beyond that inherent in our refractive index measurements.

(b) *Refractive index of polymer matrix and its temperature dependence.* We also have measured n_p and $(dn_p/dT)|_{T_0}$ for the polymer matrix material in the absence of liquid crystal.[8] The uncertainty in these measurements is ± 0.003. We have found from extensive (unpublished) measurements, however, that the index of the polymer matrix in a real PDLC film is generally not identical to the index of the cured polymer in the absence of liquid crystal. At the onset of cure, the index of the film is that of a homogeneous mixture of liquid-crystal and polymer precursors; each component contributes to the refractive index in proportion to its volume fraction in the mixture.[8] For low concentrations of liquid crystal, the contribution of liquid crystal to the index is small and the cure of the film does not depart significantly from that of the pure matrix material; in this case, the refractive index of the film increases significantly during the

TABLE II. Parameters used in computing transmittance of PDLC film by simplex minimization.

Parameter	Range	Measured/estimated value	Value from fit (independent scattering)	value from fit (with correlation)
n_{LC}	1.5784–1.5790	1.5787	1.5787	1.5789
$\left.\frac{dn_{\mathrm{LC}}}{dT}\right\|_{T_0}$	(-4.2)–$(-4.45)\times 10^{-4}\,^{\circ}\mathrm{C}^{-1}$	$-4.3\times 10^{-4}\,^{\circ}\mathrm{C}^{-1}$	$-4.20\times 10^{-4}\,^{\circ}\mathrm{C}^{-1}$	$-4.23\times 10^{-4}\,^{\circ}\mathrm{C}^{-1}$
n_p	1.555–1.573		1.565	1.557
$\left.\frac{dn_p}{dT}\right\|_{T_0}$	(-3.56)–$(-3.90)\times 10^{-4}\,^{\circ}\mathrm{C}^{-1}$		$-3.90\times 10^{-4}\,^{\circ}\mathrm{C}^{-1}$	$-3.88\times 10^{-4}\,^{\circ}\mathrm{C}^{-1}$
a	0.3–0.4 μm		0.368 μm	0.392 μm
η	0.30–0.36	≈ 0.33	0.36	0.36

cure process. For high liquid-crystal concentrations, however, the refractive index of the film changes little during the cure, at least to the point where significant phase separation and strong light scattering prevent further index measurement. These observations are consistent with calorimetric studies which suggest that the presence of liquid crystal significantly decreases the rate of matrix polymerization and that a significant fraction of the liquid crystal may remain dissolved in the matrix after cure.[2,3,10] Consequently, values of n_p and $(dn_p/dT)|_{T_0}$ in a real PDLC film cannot be determined precisely. We can say with confidence only that the refractive index of the polymer matrix in an actual PDLC film should lie between the refractive index of the starting mixture of liquid-crystal and polymer precursors and either the refractive index of the pure, cured polymer or a mixture of pure cured polymer and about 30% of the initial liquid crystal, whichever range is wider.

(c) *Film thickness.* The thickness of our PDLC film was found to be 28.27 ± 0.5 μm from analysis of the fringe spacing in its on-state transmittance versus wavelength spectrum. Determination of film thickness from fringe spacing depends on the actual value of the matrix refractive index, not on differences in index. Consequently, an uncertainty in n_p as large as 0.02 will affect the determination of d by less than 2% for values of n_p near 1.5. We fixed the thickness at its measured value throughout our computations.

(d) *Microdroplet size.* Some information about the droplet sizes in a PDLC film can be obtained from SEM photographs like the one shown in Fig. 1. However, since an SEM photograph shows a cut through a PDLC film, there would be a statistical distribution of diameters in the photograph even if all droplets were the same size. It is very difficult to extract precise information about the distribution of droplet radii from such a photograph. From Fig. 1 we can conclude, however, that there is not a wide distribution of droplet sizes in our PDLC film. Therefore, we shall assume in our calculations that all the droplets have the same radius. It is easy to show that, in this case, the droplet radius a is $4/\pi$ times the average cross-sectional radius in the photograph (≈ 0.3 μm). This corresponds to a droplet radius $a \approx 0.38$ μm.

(e) *Microdroplet volume fraction.* Table I shows that the volume fraction of liquid crystal in the mixture used to prepare our PDLC sample was 0.40. Analysis of the SEM photograph in Fig. 1 shows that, in the cured film, the droplets occupy approximately 33% of the area in the photograph. We have found from unpublished computer simulations that the volume fraction occupied by the droplets is very close to the area fraction occupied by the droplets in an SEM photograph for a variety of droplet size distributions. This means that about 20% of the liquid crystal in the starting mixture remained dissolved in the polymer matrix after polymerization. This value is consistent with the results of the calorimetric studies cited earlier.[2,3,10]

2. *Porous film of Aliev*

(a) *Liquid-crystal refractive index and its temperature dependence.* Aliev[20] recently described the temperature-

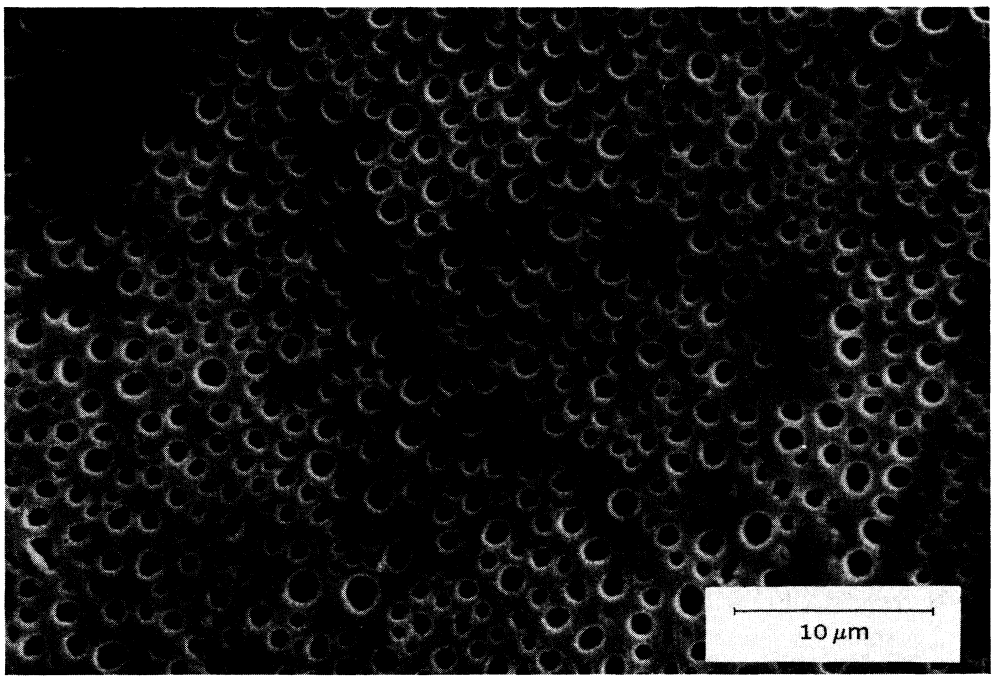

FIG. 1. Scanning electron micrograph of a cut through the PDLC film used for transmittance studies.

dependent transmittance of a porous film containing the liquid crystal cholesteryl oleate. He found that the transmittance in the isotropic phase decreased significantly with increasing temperature. Since Aliev gave no data for the refractive indices of cholesteryl oleate, we measured the index in the isotropic phase as a function of temperature using an Abbé refractometer. At 45 °C its value at 589 nm was found to be 1.4968±0.0005. This value should not differ significantly from the refractive index at 560 nm, the wavelength used by Aliev for his transmittance studies. We allowed the LC refractive index to range from 1.4963 to 1.4973 in our calculations.

To explain his transmittance data, Aliev[20] used $-2.64\times10^{-4}\,°C^{-1}$ for $(dn_{LC}/dT)|_{T_0}$, the rate of index change with temperature in the isotropic phase. Our measurements gave the value $-4.155\times10^{-4}\,°C^{-1}$, in closer agreement with typical values for liquid crystals. In our calculations, we allowed $(dn_{LC}/dT)|_{T_0}$ to range from -4.9×10^{-4} to $-2.6\times10^{-4}\,°C^{-1}$.

(b) *Refractive index of porous matrix and its temperature dependence.* Aliev's paper[20] indicates that the porous matrix material used in his liquid-crystal studies was quartz; however, further reading of the papers cited in Ref. 20 shows that the other characteristics of the porous material (pore size, volume fraction occupied by the pores, pore density, etc.), coincide exactly with those of a borosilicate glass.[26] To allow for either possibility, we let the refractive index of the matrix material vary from 1.459 to 1.528 in our calculations; for the same reason, we allowed the rate of change of this index with temperature to range from 8×10^{-6} to $1.2\times10^{-5}\,°C^{-1}$.

(c) *Film thickness.* The thickness of the Aliev sample was given as 1 mm. We fixed the thickness at this value throughout our computations.

(d) *Pore size and volume fraction.* Aliev[20] gives a pore density of 2×10^{18} cm^{-3} for his film and states that pores occupy 27% of the sample volume. If we approximate the pores as spheres, we obtain from these values an average pore diameter of 6.4 nm. This value is slightly below the 8-nm diameter given by Aliev as the peak diameter of the sharply peaked pore size distribution.[20] In our computations, we assumed spherical pores. To allow for uncertainties in pore size and volume fraction, we let the pore radius range from 3 to 4 nm and allowed the volume fraction occupied by the pores to range from 0.24 to 0.30 in our computations. By allowing these two parameters to vary independently, we allowed for large uncertainty in the pore density.

IV. RESULTS AND DISCUSSION: PDLC FILM

A. Measurement of film transmittance

Film transmittance was measured at the wavelength $\lambda=589$ nm using a Perkin-Elmer λ-5 spectrophotometer. The sample, mounted in the sample compartment of the λ-5, was heated with a hot air gun to above 90 °C. The sample compartment was then closed and the transmittance was measured at discrete temperatures as the sample cooled. Temperatures were measured with a thermocouple attached to the sample. A significant decrease in transmittance was observed when the temperature decreased below T_{NI}, the nematic-to-isotropic phase transition temperature,[27] because of the onset of scattering in the nematic phase. The solid squares in Fig. 2 are measured values of the transmittance of our PDLC sample at temperatures above T_{NI}. We estimate the uncertainty in the measured transmittance values to be about ±0.01, i.e., the error bar is essentially the size of the solid square symbols in the figure. The two main features of the transmittance data are its high (≈0.83) value and its small increase (≈0.82 to 0.84) over a 50 °C temperature range.

There appears to be a small oscillation in the transmittance data of Fig. 2 which has the appearance of an interference effect. We note that the amplitude of the oscillations is comparable to the uncertainty in the transmittance measurements so that we cannot say definitively whether the oscillations are real or an experimental artifact. We did explore in some detail the possibility that the oscillations were caused by reflection at the matrix-electrode interfaces coupled with changes in the optical thickness nd of the film as the temperature varied. It is easy to show that, if this were the case, the separation between successive maxima occurring at temperatures T and ΔT would be given by

$$\Delta T=-\left[\frac{\lambda}{2d(T)}\right]\left[\frac{dn}{dT}+(\beta_V/3)n(T)\right]^{-1}, \qquad (17)$$

where β_V is the coefficient of volume expansion of the polymer film, $n(T)$ is the film refractive index at temperature T, dn/dT is the rate of change of this index with

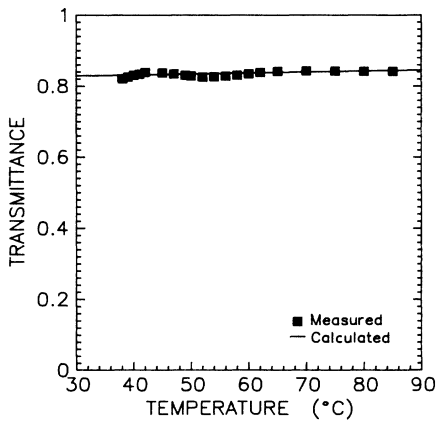

FIG. 2. Transmittance of PDLC sample of Fig. 1 vs temperature. The experimental data points are denoted by solid squares whose size denotes the uncertainty in the measured transmittance. The solid curve is calculated from Rayleigh-Gans light-scattering theory. Identical results are obtained using parameters obtained from unconstrained linear regression and by simplex minimization with film parameters constrained to be close to their experimental values.

temperature, $d(T)$ is the film thickness at temperature T, and λ is the wavelength of the light in vacuum. We found that, for any reasonable values of the parameters in Eq. (17), the computed ΔT was always at least 3.5 times larger than the measured separation (about 25 °C) between the transmittance "maxima" of Fig. 2. Since the amplitude of the oscillations is much smaller than the measured transmittance and comparable to the uncertainty in transmittance at all temperatures, we have not attempted to account for the oscillations in comparing our data with calculations.

B. Comparison of calculated and measured transmittance

Column 4 of Table II shows the film parameter values for which the constrained simplex minimization procedures discussed in Sec. III produced the best agreement between calculated and measured transmittance under the assumption that microdroplet correlation effects were unimportant [$\beta=0$ in Eq. (7)]. Using these parameters, we computed the transmittance as a function of temperature using Eq. (10). The computed curve is shown by the solid line in Fig. 2; it gives excellent agreement with the experimental data over the entire temperature range.

Column 5 of Table II shows the film parameter values for which constrained simplex minimization produced the best agreement between calculated and measured transmittance under the assumption that microdroplet correlation effects were important [$\beta=1$ in Eq. (7)]. Using these values, we computed the transmittance as a function of temperature using Eq. (10). The computed curve is indistinguishable from the solid curve in Fig. 2.

The values of liquid-crystal refractive index, of the rates of change with temperature of both the liquid-crystal and matrix refractive indices, and of the droplet volume fraction which gave the best agreement between theory and experiment were nearly identical regardless of whether or not correlation effects were taken into account. The droplet radius which gave the best results when correlation effects were included was about 6.5% larger than the radius which gave best results in the absence of correlation. This difference is well within the accuracy with which droplet sizes can be determined from scanning electron microscopy. When correlation effects were included in the calculations, the matrix refractive index which gave best results (1.557) was slightly lower than the value which gave best results in the absence of correlation (1.565). Both these values are lower than 1.5700, the refractive index of the cured matrix material in the absence of liquid crystal.[8] The value obtained with correlation is very close to the value (1.555) of the starting mixture of liquid crystal, resin, and hardener from which the film was cured. Both matrix index values are consistent with our observation that the index of a PDLC film changes very little during the cure process for droplet volume fractions comparable to that in our sample.

To explore the effect of matrix refractive index on calculated transmittance, we repeated our simplex calculations while constrainting the matrix refractive index to be equal to the index of the cured matrix material in the absence of liquid crystal (1.570 ± 0.003). In the absence of correlation, the minimization process gave the same values for droplet volume fraction, LC refractive index, and the rates of change of both the LC and matrix which had been found previously (Table II, column 4). However, it selected the smallest possible allowed matrix refractive index (1.567) and the largest allowed droplet radius (0.4 μm) in an effort to maximize scattering and reduce transmittance. Still, the calculated transmittance was about 1.5% too high. When correlation effects were included, not only did the matrix index assume its lowest allowed value and the droplet radius its largest allowed value, but the volume fraction also decreased to its lowest allowed value (this maximizes scattering when correlation effects are included); now, the calculated transmittance was about 6% too high. Had the droplet radius and volume fraction not been allowed to deviate from the best-fit values of Table II, forcing the matrix refractive index to be that of the pure cured polymer in the absence of liquid crystal would have produced even higher transmittance.

These additional computations demonstrate that the extinction cross section and, hence, the transmittance of a PDLC film, are very sensitive to the value of the matrix refractive index. They also show that, if we could more accurately measure this index in real PDLC films, transmittance measurements might be used to determine the importance of correlation effects in light scattering in PDLC films. Unfortunately, at this time there is no reliable technique for measuring the matrix refractive index in a cured PDLC film with better accuracy.

It is interesting to note that, if we compute the transmittance as a function of temperature from Eq. (13) using coefficients c_1 and c_2 obtained from an unconstrained least-squares fit of our experimental transmittance data to Eq. (16), the computed curve is indistinguishable from the solid curve in Fig. 2; thus, the best possible agreement between calculation and experiment is obtained with parameters consistent with their measured values.

V. RESULTS AND DISCUSSION: POROUS FILM OF ALIEV

The solid squares in Fig. 3 show the transmittance values reported by Aliev for a film consisting of LC material in its isotropic phase in the pores of a solid matrix.[20] We obtained these values by digitizing the curves in Aliev's paper. In contrast to the transmittance of our PDLC film, which increases slightly with increasing temperature, the transmittance of the Aliev sample decreases significantly as temperature increases.

The solid curve in Fig. 3 was computed from Eq. (13) using coefficients c_1 and c_2 obtained from an unconstrained least-squares fit of the experimental transmittance data to Eq. (16). Thus, our screening procedure (Sec. III) showed that Aliev's data are not inconsistent with the general form of the equations of RG light-scattering theory. This substantiates Aliev's conclusion[20] that, in the isotropic phase, the transmittance of his sample could be described by a temperature dependent extinction coefficient proportional to $[n_m - n(T)]^2$, where

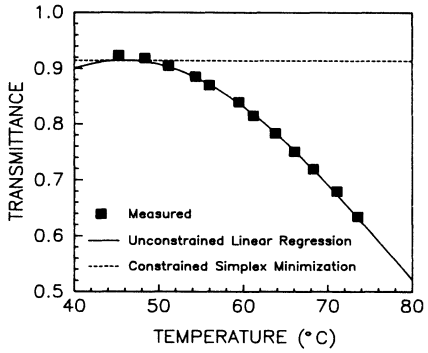

FIG. 3. Transmittance of a film consisting of liquid crystal in the pores of a solid matrix. The data points are from Ref. 20. The solid curve is a least-squares fit using parameters obtained from unconstrained linear regression. The dashed curve is calculated from simplex minimization with all film parameters constrained to be close to the values given in Ref. 20.

n_m is the refractive index of the porous matrix material (which he assumed independent of temperature) and $n(T)$ is the temperature-dependent refractive index of the liquid crystal in the isotropic phase.

As noted earlier, however, it is possible to obtain the correct temperature dependence with linear regression parameters unrelated to the real physical parameters of the system. Therefore, as we did with the PDLC film, we applied the full equation for transmittance derived from scattering theory [Eq. (10)] to the Aliev sample.

We were unable to fit the transmittance data of Fig. 3 with our simplex algorithm for any combination of parameters in the ranges given in the preceding discussion of input parameters. We always found much higher transmittance than measured experimentally, particularly at high temperatures. To understand this result, we examine Eq. (10) to determine the smallest transmittance which could be achieved using parameters characteristic of the Aliev sample. The smallest possible transmittance will be obtained by maximizing the reflectance R at the air-sample interface, the index difference $|n_{LC}-n_m|$, the function $\Phi^{\text{eff}}(ka)/a$, and the volume fraction η.

For $n_{LC}<n_m$, choosing n_m to be as large as possible will maximize both the air-sample reflectance R and the index difference $|n_{LC}-n_m|$ for any value of the liquid-crystal refractive index n_{LC} within the range used in our calculations. The maximum index difference will be obtained for the smallest liquid-crystal refractive index. Therefore, at 45 °C, we shall choose a porous matrix index $n_m=1.528$ and a liquid-crystal refractive index $n_{LC}=1.493$. To maximize the index difference at all temperatures, we shall allow n_m to increase with temperature as rapidly as possible $[(dn_m/dT)|_{T_0}=1.2\times10^{-5}\,°\text{C}^{-1}]$ and allow n_{LC} to decrease as rapidly as possible with temperature $[(dn_{LC}/dT)|_{T_0}=-4.9\times10^{-4}\,°\text{C}^{-1}]$.

The function $\Phi^{\text{eff}}(ka)/a$ increases monotonically with increasing a. Therefore, we shall choose $a=4$ nm to make this quantity as large as possible. For $\lambda=560$ nm and the refractive indices discussed above, we obtain $ka=0.068\,58$ and $\Phi^{\text{eff}}(ka)=2.621\times10^{-5}$ at 45 °C and $ka=0.068\,60$ and $\Phi^{\text{eff}}(ka)=2.624\times10^{-5}$ at 80 °C. [In these calculations, we have neglected the effects of droplet correlation; including correlation effects would reduce the value of $\Phi^{\text{eff}}(ka)$ and increase transmittance for a given radius a.]

The number of pores per unit volume and the volume fraction are related by Eq. (9). For the value of a we have chosen and the largest allowable volume fraction ($\eta=0.3$), the pore density is 1.12×10^{24} m^{-3}, about half that specified by Aliev. For this value of N_v, the computed minimum transmittance is 0.9141 at 45 °C and 0.9132 at 80 °C, as illustrated by the dashed curve in Fig. 3. (Had we required the pore density to be the Aliev value, we would have had to use a radius of 3.2 nm; this would have reduced the product $N_v\sigma_{\text{ext}}d$ by a factor of 2.1, resulting in higher transmittance.) Since extrapolation of the curve in Fig. 3 to 80 °C gives a transmittance of about 50% at that temperature, well below the minimum possible theoretical value (dashed curve), it is clear that it is impossible to explain the data of Aliev[20] from RG single-scattering theory if the parameters specified in Ref. 20 are correct.

VI. SUMMARY AND CONCLUSIONS

We have measured the transmittance of a PDLC film above the isotropic-nematic phase transition of the LC material in the microdroplets; we found it to be ~0.83 and to increase by about 1% over a 50 °C temperature range. We compared these measurements with calculations of film transmittance using RG light-scattering theory. As input parameters we used values of the LC and matrix refractive indices and their rates of change with temperature, film thickness, and LC droplet size and droplet volume fraction which had been either measured directly or estimated from experimental data. In the calculations, the parameters were allowed to vary only within their experimental uncertainties. At all temperatures, the calculated and measured transmittance values agreed to within the $\approx1\%$ experimental error in the transmittance data. No freely adjustable parameters or arbitrary normalization constants were needed to achieve this agreement between theory and experiment.

We found that, given the precision with which relevant film parameters can be determined at this time, equally good agreement between theory and experiment could be obtained by neglecting or including in our calculations correlation effects due to droplet position in the polymer matrix. The principal factor limiting our ability to determine the importance of correlation effects is the uncertainty in the refractive index of the matrix material in an actual PDLC film. Unpublished optical measurements and published calorimetric studies[2,3,10] have indicated that the refractive index of the matrix in a PDLC film may differ significantly from the index of the cured matrix material in the absence of LC; the presence of LC retards the curing process so that the refractive index of the matrix in the cured film may not increase significantly above the index of a volume-fraction-weighted mixture of

the LC and polymer precursors from which the film is formed. However, the onset of strong light scattering prevents direct measurement of the matrix index in films with LC concentrations comparable to that in our film (which is typical of PDLC films of practical interest). The values of matrix refractive index which gave best agreement with the measured transmittance data supported these ideas. We found that, if we tightly constrained the value of the matrix refractive index, the computed transmittance values with and without correlation were sufficiently different that, had we been able to determine the matrix index precisely, we would probably have been able to assess the importance of correlation effects by comparing calculated and measured transmittance values despite the uncertainties in droplet size and concentration.

We also examined the temperature-dependent transmittance of a liquid crystal in it isotropic phase in the pores of a solid transparent matrix, which had been published previously by Aliev *et al.*[20] Unlike the PDLC film transmittance, which *increased* from about 0.82 to 0.84 as the temperature was raised by about 50 °C above the isotropic-nematic transition temperature, the transmittance of the Aliev sample *decreased* sharply from about 0.9 to 0.6 for a 30 °C increase in temperature. We found, using unconstrained regression analysis, that this transmittance decrease with temperature was consistent with the general form of the equations of scattering theory, as claimed by Aliev. However, it was not possible to quantitatively describe such a large transmittance change using the published parameters for the Aliev sample, even allowing for very large uncertainties in their values. We conclude, therefore, that either the published film parameters are incorrect or there is an additional physical process occurring in this system which cannot be accounted for by scattering theory.

ACKNOWLEDGMENTS

We thank S. Žumer and J. W. Doane for useful discussions concerning the use of the radial distribution function in light-scattering calculations and for providing a copy of their recent paper (Ref. 12) prior to publication. We thank Wilson Marion for measuring the refractive indices of cholesteryl oleate and Jack Gay for supplying the simplex algorithm used in our calculations. We also thank George Smith for a critical reading of the manuscript.

APPENDIX A: TRANSMITTANCE OF A SYSTEM OF LIGHT-SCATTERING RAYLEIGH-GANS PARTICLES: CORRELATION EFFECTS

Standard texts on light scattering[16–18] generally assume that the power scattered by a system of identical particles is the power scattered by one particle times the number of particles which interact with the incoming light beam. This assumption neglects the fact that, if the positions of all the particles are referred to a common origin, the scattered field at position $\mathbf{r}$ produced by a particle at position $\mathbf{r}_i$ will differ by a phase factor from the scattered field produced at $\mathbf{r}$ by an identical particle at the origin. The situation is illustrated in Fig. 4 which shows light propagating in the direction specified by wave vector $\mathbf{k}$ being scattered in the direction specified by wave vector $\mathbf{k}'$ by a particle at the origin and by a second, identical particle at $\mathbf{r}_i$. It is clear from geometry that, *if the assumptions required for validity of the RG approximation are satisfied* [see Eqs. (1) and (2) of the text], the scattered field produced by the particle at $\mathbf{r}_i$ will be shifted in phase from that produced by the particle at the origin by an amount $\mathbf{k}_s \cdot \mathbf{r}_i$, where $\mathbf{k}_s = \mathbf{k} - \mathbf{k}'$. In other words, the scattered field produced at position $\mathbf{r}$ by particle i at position $\mathbf{r}_i$ will be the field $\mathbf{E}_i(\mathbf{r})$, which would be produced at $\mathbf{r}$ if the particle were located at the origin, times a phase factor $\exp(i\mathbf{k}_s \cdot \mathbf{r}_i)$.

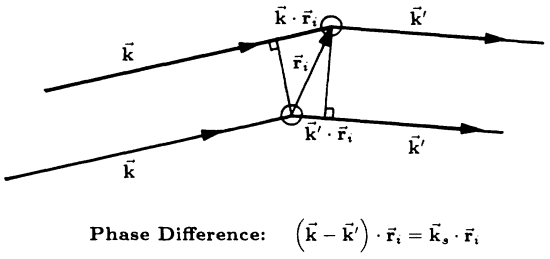

FIG. 4. Diagram showing the phase difference in the scattered electric fields produced by a Rayleigh-Gans particle at the origin and a second, identical particle at $\mathbf{r}_i$.

In this appendix we derive an expression for the scattering cross section for a system of N scatterers, taking into account the phase relationships between the scattered electric fields produced by the individual particles. Our approach is similar to that used in texts on statistical mechanics for describing the scattering of light and x rays by density fluctuations is gases and liquids.[28]

The total scattered field produced by a system of particles is the sum of the fields scattered by the individual particles,

$$\mathbf{E}_{sN}(\mathbf{r}) = \sum_{i=1}^{N} \mathbf{E}_i(\mathbf{r}) e^{i\mathbf{k}_s \cdot \mathbf{r}_i} \tag{A1}$$

and

$$|\mathbf{E}_{sN}(\mathbf{r})|^2 = \left[\sum_{i=1}^{N} \mathbf{E}_i(\mathbf{r}) e^{i\mathbf{k}_s \cdot \mathbf{r}_i} \right] \cdot \left[\sum_{j=1}^{N} \mathbf{E}_j(\mathbf{r}) e^{i\mathbf{k}_s \cdot \mathbf{r}_j} \right]^* . \tag{A2}$$

If all the particles are not identical, the term $\mathbf{E}_i(\mathbf{r})$ will be different for each particle; for identical particles, $\mathbf{E}_i(\mathbf{r})$ will be the same for all particles in the system.

Equation (A2) may be written

$$|\mathbf{E}_{sN}(\mathbf{r})|^2=\int_V d\mathbf{r}'\int_V d\mathbf{r}''\sum_{i,j=1}^{N}\mathbf{E}_i(\mathbf{r})\cdot\mathbf{E}_j^*(\mathbf{r})e^{i\mathbf{k}_s\cdot(\mathbf{r}'-\mathbf{r}'')}\delta(\mathbf{r}'-\mathbf{r}_i)\delta(\mathbf{r}''-\mathbf{r}_j)\ . \tag{A3}$$

In the remainder of this section we shall assume that all the particles are identical so that

$$\mathbf{E}_i(\mathbf{r})=\mathbf{E}_j(\mathbf{r})=\mathbf{E}_s(\mathbf{r})\ , \tag{A4}$$

where $\mathbf{E}_s(\mathbf{r})$ is the scattered field produced at position $\mathbf{r}$ by one of the identical particles located at the origin. For a spherical scatterer of radius a illuminated by unpolarized light, $|\mathbf{E}_s|^2$ is given in the RG approximation by[16]

$$|\mathbf{E}_s|^2=\frac{1+\cos^2\theta_s}{8\pi^2r^2}k^4V_p^2|m-1|^2|R|^2|\mathbf{E}_0|^2\ , \tag{A5}$$

where V_p is the volume of the scatterer, $m=n/n_m$, $\mathbf{E}_0$ is the incident electric field, and

$$R=\frac{3}{(k_sa)^3}(\sin k_sa-k_sa\cos k_sa)\ . \tag{A6}$$

Using this result, and taking an ensemble average, we obtain from Eq. (A3)

$$\langle|\mathbf{E}_{sN}(\mathbf{r})|^2\rangle=|\mathbf{E}_s(\mathbf{r})|^2\int_V d\mathbf{r}'\int_V d\mathbf{r}''e^{i\mathbf{k}_s\cdot(\mathbf{r}'-\mathbf{r}'')}\left\langle\sum_{i,j=1}^{N}\delta(\mathbf{r}'-\mathbf{r}_i)\delta(\mathbf{r}''-\mathbf{r}_j)\right\rangle\ . \tag{A7}$$

The angular brackets in this equation denote the ensemble average.

Since the number density of particles $n(\mathbf{r})$ may be written as

$$n(\mathbf{r})=\sum_{i=1}^{N}\delta(\mathbf{r}-\mathbf{r}_i)\ , \tag{A8}$$

the ensemble average in the integrand of Eq. (A7) is $\langle n(\mathbf{r}')n(\mathbf{r}'')\rangle$, the density-density correlation function.[29] In dealing with this function, it is convenient to treat the $i=j$ term in the summation separately from the terms with $i\neq j$. It is straightforward to show, using the properties of δ functions, that the $i=j$ term gives $\langle N\rangle$, the average number of particles in the scattering volume V.

The ensemble average of the summation for $i\neq j$ is $n^{(2)}(\mathbf{r},\mathbf{r}')$, the two particle density[30] (sometimes called the probability density for pairs or pair distribution function). Physically, $n^{(2)}(\mathbf{r},\mathbf{r}')d\mathbf{r}\,d\mathbf{r}'$ is the probability of finding one particle in the volume element $d\mathbf{r}$ at $\mathbf{r}$ and a second particle in the volume element $d\mathbf{r}'$ at $\mathbf{r}'$. The two particle density is related to the radial distribution function $g(\mathbf{r},\mathbf{r}'-\mathbf{r})$ by[28]

$$n^{(2)}(\mathbf{r},\mathbf{r}')=\langle n\rangle^2g(\mathbf{r},\mathbf{r}'-\mathbf{r})\ , \tag{A9}$$

where $\langle n\rangle$ is the ensemble average of the number density $n(\mathbf{r})$; $\langle n\rangle$ is, of course, the quantity which we have denoted previously by N_v. In isotropic media, $g(\mathbf{r},\mathbf{r}'-\mathbf{r})$ depends only on the interparticle separation $|\mathbf{r}'-\mathbf{r}|$.[28,30] Using this result we obtain, after a change of variable and some manipulation,

$$\langle|\mathbf{E}_{sN}(\mathbf{r})|^2\rangle=\langle N\rangle|\mathbf{E}_s(\mathbf{r})|^2\times\left[1+N_v\int_V d\mathbf{r}'\,e^{i\mathbf{k}_s\cdot(\mathbf{r}')}g(r')\right]\ . \tag{A10}$$

Let us write

$$\int_V d\mathbf{r}'e^{i\mathbf{k}_s\cdot(\mathbf{r}')}g(r')=\int_V d\mathbf{r}'e^{i\mathbf{k}_s\cdot(\mathbf{r}')}+\int_V d\mathbf{r}'e^{i\mathbf{k}_s\cdot(\mathbf{r}')}[g(r')-1]\ . \tag{A11}$$

Consider the phase term $\mathbf{k}_s\cdot\mathbf{r}'$ in the first integral. The wave vector $\mathbf{k}_s$ has magnitude $(4\pi n_m/\lambda)\sin\theta_s/2$. For 589-nm light in a medium with refractive index $n_m=1.5$, $4\pi n_m/\lambda\approx32\ \mu\text{m}^{-1}$. This means that the phase $\mathbf{k}_s\cdot\mathbf{r}'$ will oscillate rapidly during integration over the sample volume and the integral will be ≈0 unless the scattering angle θ_s is very small ($\approx0.1°$). Light within this small cone is indistinguishable experimentally from unscattered transmitted light and does not contribute to scattering of energy out of the incident beam. Therefore, the first integral on the right-hand side of Eq. (A11) does not contribute to the scattered electric field.

In the second integral, the factor $g(r')-1$ approaches 0 for large interparticle separations; therefore, we can extend the volume of integration to infinity and the second integral becomes the Fourier transform of $[g(r')-1]$. Using these results in Eq. (A10) and taking into account the relation[13]

$$|\mathbf{E}_s|^2=\frac{1}{r^2}\frac{d\sigma}{d\Omega}|\mathbf{E}_0|^2 \tag{A12}$$

between the absolute square of the scattered electric field and the differential scattering cross section of a particle, we obtain the differential scattering cross section $[d\sigma/d\Omega]_N$ for the system of N identical particles,

$$\left[\frac{d\sigma}{d\Omega}\right]_N=N\left[\frac{d\sigma}{d\Omega}[1+N_v\hat{h}(k_s,\eta,a)]\right]=N\frac{d\sigma^{\text{eff}}}{d\Omega}\ , \tag{A13}$$

where $\hat{h}(k_s,\eta,a)$, the Fourier transform of $h(r')=g(r')-1$, is given by

$$\hat{h}(k_s,\eta,a)=\int_V d\mathbf{r}' e^{i\mathbf{k}_s\cdot(\mathbf{r}')}h(r') =4\pi\int_0^\infty r'^2 h(r')\frac{\sin k_s r'}{k_s r'}dr' . \quad \text{(A14)}$$

We have, for convenience in notation, dropped the angular brackets denoting the ensemble average. We have also indicated explicitly that the term $\hat{h}(k_s,\eta,a)$ may depend on the radius and volume fraction of the scatterers (see Appendix B).

Equation (A13) defines an effective differential scattering cross section per particle, $d\sigma^{\text{eff}}/d\Omega$, when correlation effects are included. It consists of two parts:

(1) The differential cross section of a single particle $d\sigma/d\Omega$. This is the independent scattering contribution. In the absence of correlation effects, the differential cross section for the N particle system is just this term multiplied by N.

(2) The correlation term $(d\sigma/d\Omega)N_v\hat{h}(k_s,\eta,a)$. This term takes into account the phase relations in the scattered field which depend on particle position within the sample.

The effective total scattering cross section per particle, including correlation effects, is obtained by integration of the effective differential cross section per particle over all solid angles. Using Eqs. (A5), (A6), (A12), and (A13), we may write it in the form

$$\sigma_s^{\text{corr}}=\pi a^2|m-1|^2\Phi^{\text{corr}}(ka) , \quad \text{(A15)}$$

where

$$\Phi^{\text{corr}}(ka)=\tfrac{4}{9}(ka)^4\int_0^\pi(1+\cos^2\theta_s)\left[\frac{3}{(k_sa)^3}(\sin k_sa-k_sa\cos k_sa)\right]^2[1+N_v\hat{h}(k_s,\eta,a)]\sin\theta_s d\theta_s . \quad \text{(A16)}$$

If the factor $[1+N_v\hat{h}(k_s,\eta,a)]$ in Eq. (A16) is replaced by unity, we recover the function $\Phi(ka)$ which describes independent scattering by a single sphere in the RG approximation.[16] Thus, the extinction cross section σ_{ext} of a single, nonabsorbing RG sphere may be written in the general form

$$\sigma_{\text{ext}}=\sigma_s^{\text{eff}}=\pi a^2|m-1|^2\Phi^{\text{eff}}(ka) , \quad \text{(A17)}$$

with

$$\Phi^{\text{eff}}(ka)=\tfrac{4}{9}(ka)^4\int_0^\pi(1+\cos^2\theta_s)\left[\frac{3}{(k_sa)^3}(\sin k_sa-k_sa\cos k_sa)\right]^2[1+\beta N_v\hat{h}(k_s,\eta,a)]\sin\theta_s d\theta_s . \quad \text{(A18)}$$

The factor β in Eq. (A18) is given by

$$\beta=\begin{cases}0, & \text{for independent scattering (no correction effects) ;}\\ 1, & \text{if droplet correlation effects are important .}\end{cases} \quad \text{(A19)}$$

In Appendix B, we use the Percus-Yevick approximation for hard spheres[21] to obtain explicit expressions for $\hat{h}(k_s,\eta,a)$ for use in our calculations.

APPENDIX B: FOURIER TRANSFORM OF THE RADIAL DISTRIBUTION FUNCTION FOR HARD SPHERES IN THE PERCUS-YEVICK APPROXIMATION

In Appendix A, we wrote the effective differential and total scattering cross sections for a system of particles in terms of a function $\hat{h}(k_s,\eta,a)$, the Fourier transform of $h(r)=g(r)-1$, where $g(r)$ is the radial distribution function for the system. The radial distribution function depends on the potential energy function which describes the interaction between the particles in the system. For a PDLC film containing spherical droplets of uniform size, it is reasonable to describe the system as a collection of hard spheres of radius a. Of the many approaches which have been used to calculate the radial distribution function for hard spheres, we choose the Percus-Yevick (PY) approximation[21] for our calculations. The radial distribution function for hard spheres computed with the PY formalism agrees very well with that obtained from computer simulations[21] (molecular-dynamics and Monte Carlo calculations), which are known to be the most accurate procedures for computing radial distribution functions.[31] Since the PY approximation is valid even at high particle density, we can legitimately apply it to the relatively high droplet concentrations found in many PDLC films.

Of particular interest for this work is the fact that, although computation of the hard-sphere radial distribution function in the PY approximation is complicated, computation of its Fourier transform is quite simple. The Fourier transform $\hat{h}(k_s,\eta,a)$, is related to $\hat{c}(k_s,\eta,a)$, the Fourier transform of the direct correlation function $c(r)$,[21]

$$\hat{h}(k_s,\eta,a)=\frac{\hat{c}(k_s,\eta,a)}{1-N_v\hat{c}(k_s,\eta,a)} . \quad \text{(B1)}$$

In the PY approximation, the direct correlation function $c(r)$ for hard spheres has the form[32]

$$c(r)=-\lambda_1-6\eta\lambda_2(r/D)-\tfrac{1}{2}\eta\lambda_1(r/D)^3, \quad r\le D$$
$$c(r)=0, \quad r>D \quad \text{(B2)}$$

where $D=2a$ is the diameter of a droplet, η is the volume fraction occupied by the droplets, and λ_1 and λ_2 are given by[32]

$$\lambda_1=\frac{(1+2\eta)^2}{(1-\eta)^4}\ ,$$
$$\lambda_2=-\frac{(1+\frac{1}{2}\eta)^2}{(1-\eta)^4}\ . \tag{B3}$$

The Fourier transform $\hat{c}(k_s,\eta,a)$ is given by

$$\hat{c}(k_s,\eta,a)=D^3(\hat{c}_1+\hat{c}_2+\hat{c}_3)\ , \tag{B4}$$

where

$$\hat{c}_1=-\frac{4\pi\lambda_1}{\phi_{ks}^3}(\sin\phi_{ks}-\phi_{ks}\cos\phi_{ks})\ ,$$
$$\hat{c}_2=-\frac{24\pi\eta\lambda_2}{\phi_{ks}^4}[2\phi_{ks}\sin\phi_{ks}-(\phi_{ks}^2-2)\cos\phi_{ks}-2]\ ,$$
$$\hat{c}_3=-\frac{2\pi\eta\lambda_1}{\phi_{ks}^6}[(-\phi_{ks}^4+12\phi_{ks}^2-24)\cos\phi_{ks}+(4\phi_{ks}^3-24\phi_{ks})\sin\phi_{ks}+24]\ . \tag{B5}$$

In this equation, we have introduced the dimensionless variable $\phi_{ks}=k_sD$.

[1]J. W. Doane, N. A. Vaz, B.-G. Wu, and S. Žumer, Appl. Phys. Lett. **48**, 269 (1986).

[2]Nuno A. Vaz, George W. Smith, and G. Paul Montgomery, Jr., Mol. Cryst. Liq. Cryst. **146**, 1 (1987).

[3]Nuno A. Vaz, George W. Smith, and G. Paul Montgomery, Jr., Mol. Cryst. Liq. Cryst. **146**, 17 (1987).

[4]Paul S. Drzaic, J. Appl. Phys. **60**, 2142 (1986).

[5]G. Paul Montgomery, Jr. and Nuno A. Vaz, Appl. Opt. **26**, 738 (1987).

[6]Peter van Konynenburg, Stephen Marsland, and James McCoy, Proc. SPIE **823**, 143 (1987).

[7]J. W. Doane, A. Golemme, J. L. West, J. B. Whitehead, Jr., and B.-G. Wu, Mol. Cryst. Liq. Cryst. **165**, 511 (1988).

[8]Nuno A. Vaz and G. Paul Montgomery, Jr., J. Appl. Phys. **62**, 3161 (1987).

[9]Bao-Gang Wu, John L. West, and J. William Doane, J. Appl. Phys. **62**, 3925 (1987).

[10]G. Paul Montgomery, Jr., Nuno A. Vaz, and George W. Smith, Proc. SPIE **958**, 104 (1988).

[11]S. Žumer and J. W. Doane, Phys. Rev. A **34**, 3373 (1986).

[12]S. Žumer, A. Golemme, and J. W. Doane, J. Opt. Soc. Am. A **6**, 403 (1989).

[13]S. Žumer Phys. Rev. A **37**, 4006 (1988).

[14]J. B. Whitehead, Jr., S. Žumer, and J. W. Doane, Proc. SPIE **1080**, 250 (1989).

[15]R. D. Sherman, Phys. Rev. A **40**, 1591 (1989).

[16]H. C. van de Hulst, *Light Scattering by Small Particles* (Wiley, New York, 1957).

[17]M. Kerker, *The Scattering of Light and Other Electromagnetic Radiation* (Academic, New York, 1969).

[18]C. F. Bohren and D. R. Huffman, *Absorpton and Scattering of Light by Small Particles* (Wiley, New York, 1983).

[19]G. Paul Montgomery, Jr., J. Opt. Soc. Am. B **5**, 774 (1988).

[20]F. M. Aliev, Pis'ma Zh. Eksp. Teor. Fiz. **41**, 254 (1985) [JETP Lett. **41**, 310 (1985)].

[21]See, for example, H. Eyring, D. Henderson, B. J. Stover, and E. M. Eyring, *Statistical Mechanics and Dynamics* (Wiley, New York, 1982).

[22]7CB is an abbreviation for [1,1′−Biphenyl]·4 carbonitrile, 4′ heptyl. This material is available from E. M. Chemicals, Hawthorne, New York.

[23]Available from Devcon Corp., Danvers, MA.

[24]This 40% figure assumes that the matrix behaves as pure cured polymer with n_p and $(dn_p/dT)|_{T_0}$ given in Table I. This value will change as n_p and $(dn_p/dT)|_{T_0}$ change but, for any reasonable values of these parameters, the $(n_{LC}-n_p)$ factor will still dominate the temperature dependence of the extinction coefficient.

[25]J. A. Nelder and R. Mead, Comp. J. **7**, 308 (1965).

[26]V. I. Zemskiĭ, I. K. Meshovskiĭ, and A. V. Sechkarev, Dokl. Acad. Nauk USSR **267**, 1377 (1982) [Sov. Phys. Dokl. **27**, 1047 (1982)].

[27]The measured value of T_{NI} in our PDLC film was 37.5 °C. This value is slightly lower than the 42.8 °C value of T_{NI} supplied by the manufacturer for the pure liquid crystal 7CB (Ref. 22). Such depressions of T_{NI} are commonly observed in PDLC films, as discussed in Refs. 1, 2, and 10.

[28]J. O. Hirschfelder, C. F. Curtiss, and R. B. Bird, *Molecular Theory of Gases and Liquids* (Wiley, New York, 1954).

[29]C. V. Heer, *Statistical Mechanics, Kinetic Theory, and Stochastic Processes* (Academic, New York, 1972).

[30]M. Toda, R. Kubo, and N. Saito, *Statistical Physics I Equilibrium Statistical Mechanics* (Springer-Verlag, Berlin, 1983).

[31]J. A. Barker and D. Henderson, Rev. Mod. Phys. **48**, 587 (1976).

[32]M. S. Wertheim, J. Math. Phys. **5**, 643 (1964).

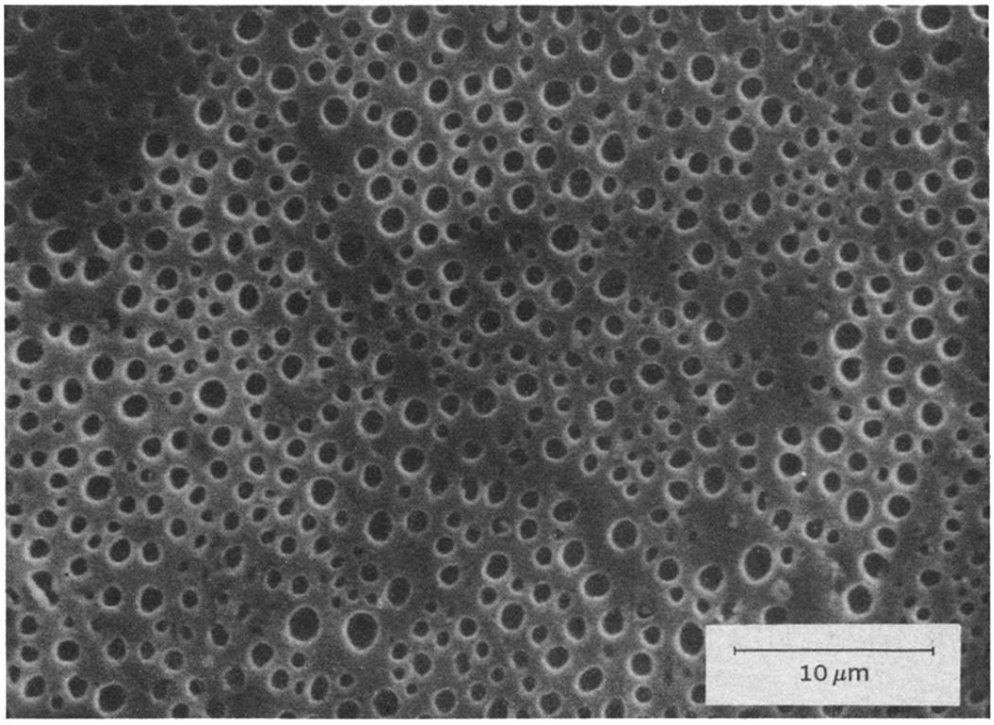

FIG. 1. Scanning electron micrograph of a cut through the PDLC film used for transmittance studies.